Atmos. Chem. Phys. Discuss., 9, 13177–13198, 2009
www.atmos-chem-phys-discuss.net/9/13177/2009/

Atmospheric
Chemistry
and Physics
Discussions

Patterns of Saharan dust transport over the Atlantic: winter vs. summer, based on CALIPSO first year data

B. A. Yuval, K. Ilan, and A. Orit

Department of Environmental Sciences and Energy Research, Weizmann Institute of Science, Rehovot, Israel

Received: 20 April 2009 – Accepted: 26 May 2009 – Published: 15 June 2009

Correspondence to: B. A. Yuval (yuval.ben-ami@weizmann.ac.il)

Published by Copernicus Publications on behalf of the European Geosciences Union.

Abstract

One of the most important factors that determines the transported dust effect is its vertical distribution in the atmosphere. Until the launch of the Cloud-Aerosol Lidar and Infrared Pathfinder Satellite Observation (CALIPSO), the vertical distribution was studied mostly by in-situ measurements and models. CALIPSO, as a part of the A-Train constellation has opened an opportunity to study the transported dust vertical structure in a large number of events (sufficient statistics).

In this study the vertical structure of Saharan dust and stratiform clouds is analyzed over the Atlantic Ocean for the 2006–2007 winter (December–February) and the summer of 2006 (June–August). By using CALIPSO backscatter measurements over the dust route, we describe the differences in dust transport between the seasons. We show a bi-modal distribution of the average dust plumes height in both seasons (it is less clear in the winter). It suggests that a significant part of the dust is transported near and within the marine boundary layer and interacts with shallow clouds on both seasons.

1 Introduction

Mineral dust has a significant role in the natural system. Dust particles interact directly with electromagnetic radiation and therefore alter the surface-atmospheric radiation budget (Ramanathan et al., 2001; Kaufman et al., 2002; Yu et al., 2006). By serving as clouds drops/ice crystals condensation/freezing nuclei dust may indirectly invigorate convective clouds height (Koren et al., 2005) or accelerate precipitations (Levin et al., 1996), and it can also change clouds lifetime, and albedo (Albrecht, 1989; Hansen et al., 1997; Twomey, 1974; Kaufman et al., 2005a). Solar energy absorbed by dust may change the atmospheric temperature profile and therefore change cloudiness (Hansen et al., 1997). After sinking or scavenging, dust can supply essential minerals to the biosphere such as in the Amazon rain forest (Swap et al., 1992; Reichholf, 1986; Koren et al., 2006) and phytoplankton in the oceans, hence it may enhance the reduction in atmospheric CO_2 (Falkowski et al., 1998) and it can modify the ocean albedo. Dust can also decrease snow and ice albedo and enhance their melting (Psenner, 1999). It may serve as a vehicle for cross oceans transfer of fungi or bacteria, and can be associated with human diseases or oceans catastrophes (Garrison et al., 2003). Nevertheless, our knowledge on basic questions concerning the dust loading (Tanaka, 2008) and sink (Bergametti and Dulac, 2008), as well as its chemical (Engelstaedter et al., 2006) and radiative (IPCC, 2007; Wendisch et al., 2008) properties, still lack with large uncertainty.

Previous remote sensing studies (e.g.: Herman et al., 1997; Prospero et al., 2002; Israelevich et al., 2002; Middleton and Goudie, 2001, Kaufman et al., 2005b) and observations (e.g.: Prospero and Lamb, 2003) identified that the North African dust activity is subjected to a strong seasonal cycle. As a consequence, the location of the dust sources, their activity pattern and the transport routes are affected.

The synoptic conditions over West of Africa and the mid Atlantic during the summer months were discussed in details in previous studies (Karyampudi and Carlson, 1988, Karyampudi et al., 1999). The dust outbreaks occur predominantly within the ridge region of passing easterly wave disturbances with a periodicity of 5–7 days (Prospero and Carlson, 1972). These dust outbreaks occur under the conditions of a thermal low that prevails over West Africa (centered around 17°–23° N) in this period (due to intense solar heating). The converging strong low-level flow around the low lifts the dust as a result of strong surface pressure gradient. Over this region there is a deep mixed layer that often extends up to 5–6 km in height. The airborne dust is carried westward in the Saharan Air Layer (SAL) between 1.5 to 5–7 km by the prevailing easterly flow in these latitudes (Prospero and Carlson, 1972; Karyampudi et al., 1999; Karyampudi and Carleson, 1988; Prospero and Nees, 1977). Recent study proposed that the dust may extend up to 8 km (Generoso et al., 2008). Over the ocean, at low level (beneath the SAL), there are relatively clean northeasterly trade winds in the marine mixed layer. The southern equatorial trough or Intertropical Convergence Zone

(ITCZ) is located between 5°–10° N. In accordance with the meridional temperature gradient at mid levels heights, between the warm Saharan air and the cooler air in the equatorial zone, there is a strong vertical shear in the zonal wind between 850 and 650 mb, that manifests itself as a mid-level easterly jet (Karyampudi and Carlson, 1988). The 700 mb level winds represent this mid-level flow. Figure 1 presents the mean winds in the 700 mb level during the studied summer months. During these months the dust is mainly transported over the Atlantic Ocean towards the southern part of the United States, Caribbean and the north part of South-America. Often, it can be transported northerly by anticyclonic eddies over the Canaries or Azores Islands (Carlson and Prospero, 1972; Kaufman et al., 2005b).

The synoptic condition over the region during the winter months are less discussed in the literature. The synoptic systems move southward compared to the summer and they are less well defined. The thermal low over Africa is less well defined and is centered on latitudes 5°–10° N. The mid-level jet location is around 5° S–7° N. Figure 1 presents the mean wind direction in the 700 mb height during the studied winter months. The emitted dust is restricted to lower altitudes (∼1.5–3.5 km) due to westerly winds from above (Chiapello et al., 1995). It is transported south westward, toward the northern part of South America, while crossing the African coastline near the equator (Prospero et al., 2002).

During the winter months the West African Sahelian region is characterized by large areas of biomass burning fires mainly due to agricultural activities. In the same time low level easterly and north-easterly Harmattan winds transport the Saharan dust toward the biomass burning regions causing unavoidable external mixing. Ground based and aircraft measurements from the African Monsoon Multidimensional Analyses (AMMA) and the Dust Outflow Deposition to the Ocean (DODO) field experiments showed that the atmospheric column may have multi layers structure of low level dust layer and elevated biomass burning layer that contains dust as well external mixing of both aerosols. Moreover, they estimated the contribution of the dust to the elevated biomass burning aerosol layer to be extremely high (72±16%, Formenti et al., 2008). Therefore, during the winter we describe the transport of plumes of dust-biomass burning aerosol mixture.

In this study we use the attenuation backscatter measurements, done by the Cloud-Aerosol Lidar with Orthogonal Polarization (CALIOP) instrument on board the CALIPSO (Winker and Pelon, 2003) as part of the A-Train constellation (since 2006) (Anderson et al., 2005). We characterize the average dust vertical distribution in the summer (2006) versus the dust and smoke in the winter (2006–2007). We examine the dust and the stratiform clouds relative height to understand what type of interaction should be expected there.

2 Methods

The measurements made by the CALIOP instrument are three calibrated lidar profiles: total attenuated backscatter at 532 nm and 1064 nm, and the perpendicular polarization component of the backscatter at 532 nm. The vertical resolution of the 532 nm and 1064 nm channels (in the lowest 8.2 km) are 30 and 60 m respectively. Both channels have horizontal resolution of 33 km (Winker et al., 2007; Vaughan et al., 2004).

The polarization backscatter data attributed from CALIOP instrument can add significant information on aerosol shape and optical properties that can be used for aerosol classification. However, the noise level of most of the attenuated backscatter data was too high for (a) detecting the boundaries of the aerosol layer, and (b) to determining if we see smoke only, dust only or mixture. Classification process, based on this data, may not be robust. Moreover several recent papers suggested that over the ocean most of the aerosol packages are mixed.

For fast classification between aerosol and clouds and in order to mark the top and bottom of the dust layer, we hoped to use the CALIPSO Vertical Feature Mask (VFM, Vaughan et al, 2004). However we found out that for such detailed analysis the best results are obtained when the final aerosol layer is mask manually on each profile. We used the VFM as the source for the initial classifications following by manual inspection to smooth the aerosol layer (mostly in cases when clouds are embedded inside it) and taking out small patches when the confidence level is low. The classification is based on the different backscatter patterns between clouds and aerosol. While aerosol plumes have relative weak but uniform, stratiform (low, marine stratocumulus or higher stratus) clouds has a much stronger and narrower backscatter signal and convective clouds has patchy backscatter pattern. The total attenuated backscatter at 532 nm data has shown the best contrast and served as the main reference data for classification.

The selected research area is between 40° N to 20° S, and 15° E to 70° W, during 2006 summer (June–August) and 2006–2007 winter (December–February). The selection of the area was based on the dust signature on the MODIS total Aerosol Optical Depth (AOD) and aerosol fine fraction maps (Kaufman et al., 2005c) and in agreement with the dust distribution in previous studies (e.g.: Herman et al., 1997; Prospero et al., 2002).

MODIS aerosol fine mode fraction of optical depth is defined as the fraction of the total optical depth attributed to the fine mode (aerosol with diameter smaller than 1 μm) (Kaufman et al., 2005b). The fine mode fraction parameter enables discrimination between dust or sea-salt and pollution or biomass burning aerosols. Dust aerosol is dominated by large particles (diameter larger than 1 μm) and therefore will have a significant coarse mode fraction where the smoke from biomass burning and industrial aerosol are dominated by smaller particles (diameter smaller then 1 μm) and therefore are characterized by the fine mode fraction (Dubovik, et al., 2002).

The summer dust transport route is clearly shown in an area characterized by high AOD levels and low fine fraction values (Fig. 2, upper row). The winter dust transport (Fig. 2, lower row) is known to migrate southward to the border of the Sahara and the Sahel region (Kaufman et al., 2005b), where intensive biomass burning occurs. Therefore the coarse mode contribution of the dust is smoothed by the smoke, resulting in a blurrier coarse mode signature of the dust. Nevertheless, the high AOD area of the winter flux is shown to have lower fine mode values surrounded by higher fine-fraction contributed by smoke from the southern parts of Africa and Brazil and pollution form

North America.

Based on this MODIS data and taking into account the above field experiments results we decided not to distinguish between the dust and the smoke plumes during the winter. Therefore, for the winter analysis, we study the transport of a joint dust-smoke plumes.

For each backscatter vertical profile within the research area the top and the base of the aerosol plumes as well as the location of the stratiform clouds were picked (the stratiform clouds are too thin to determine their base and top heights separately). An example for the differences between the aerosol and cloud signature can be seen in Fig. 3.

When the location of the dust plume base was close to the top of the MBL, we couldn't determine its exact location. Therefore, results of plume bases height and thickness (mainly during the winter lower plumes) may introduce large error. Since the daytime measured data has higher level of noise due to the solar radiation (Liu et al., 2008) the aerosol signal in daytime profiles was enhanced by averaging the nearest 5 pixels (total of 1.65 km) along the horizontal dimension of the profile. The collected data of aerosol plumes and clouds heights, as well as the MBL depth, for both daytime and nighttime were sorted into 1°×1° grid. The data was collected from 381 daytime and 499 nocturnal CALIPSO tracks.

To avoid statistical biases in areas with rare aerosol and clouds measurements, aerosol and cloud grid points with only one daily sample were removed from the dataset. Next, the average heights of the dust and dust-smoke plumes (and clouds) were defined statistically by analyzing the local top height distribution (see a detailed description in Sects. 3.1 and 3.2).

3 Results

3.1 Dust

Analyzing the aerosol plumes top height distribution reveals a bi-modal distribution in the summer. In the winter distribution there is a dominant dust-smoke high level plumes with a minor peak in lower altitudes (Fig. 4). The low altitude mode in both seasons contains marine aerosol beside the dust. Note that although the MBL depth (often the top of the layer is bounded by marine stratocumulus clouds (MSc), see Sect. 3.2 and Fig. 3) appears in the histograms of the dust layers top height, it was excluded from the dataset in the next steps of the analysis.

In order to analyze the height distribution of the apparent bi modal distribution, we needed to separate the two modes. The best threshold for separation (after excluding the MBL samples) top heights was determined by looking for the threshold that will show the weakest sensitivity of the average top height to small threshold changes. Namely, we calculated the mean (low and high) dust top height (H_l and H_h) for a range of thresholds (Tr) and the best threshold was determined by minimizing the top's height derivatives,

$$\min\left\{\frac{dH_{l,h}}{dTr}\right\}. \tag{1}$$

From the above distribution analysis, the chosen thresholds for the aerosol average top heights are: 1) an upper aerosol plumes with top height above 2.7 and 1.6 km in the summer and winter respectively; 2) a lower aerosol plumes with top height above the MBL (0.8 km, measured by the MSc height, see Sect. 3.2) in both seasons and top height equal or below 2.7 and 1.6 km for the summer and winter, respectively.

The analysis of the dust plumes over western parts of the Atlantic Ocean reveals that the separation between the two modes is less clear. Therefore, the Region Of Interest (ROI) was selected to be the first 50° longitude from the African coastline over the Ocean (along the contours of Fig. 2).

Upper plumes: The dust top height distribution analysis along the longitudinal cross-section of the ROI, (Fig. 5a), shows that during the summer the average top height, when crossing the African coastline, is 5.1±0.4 km. During the winter the upper dust-smoke plumes are lower and the mean height near the African coastline is 3.7±0.4 km. As the upper dust plumes are transported westward they decrease in height on an average of 0.028 km per 1° longitude (slop of −0.023) during the summer and 0.02 km (slop of −0.02) during the winter. Examination of the upper dust plumes average thickness (calculated as the difference between each plume top height and its corresponding base height along the ROI, Fig. 5a) showed that on average, the upper plumes are significantly thicker during the summer (3 to 3.6 km in the summer, versus 2 to 2.7 km in the winter).

Lower plumes: Analysis of the lower dust plumes mean top height (along the ROI) shows an inverse trend (Fig. 5b), namely the dust crosses the African coastline near 1.5 and 1 km in the summer and winter respectively, and the average height increases (in an order of a few hundred meters) toward the western side of the Atlantic Ocean (in the winter the trend is less pronounced).

Comparing the seasonal spatial structure of the averaged dust plumes top height (Fig. 6a and b) to the structure of the MODIS AOD measurements over the Atlantic Ocean (Fig. 2, left panel) shows that during the summer, the maximal top height of the upper dust plumes is located north to the maximal AOD. Similar analysis of the winter season reveals that the location of the maximum top height of the dust-smoke plumes is located south to the maximal AOD location. A possible explanation to this difference is the African relief that may serve as an orographic barrier that lifts the transported dust: during the summer it may be the Atlas mountains, located in the north western part of Africa (Morocco, Algeria, and Tunisia), while in the winter the transported dust may be lifted by mount Oku (3000 m) and mount Cameroon (4070 m), both located in Cameroon. Note that the MODIS winter fine fraction distribution (Fig. 2, lower right side) shows higher fine fraction values in the southern region suggesting a larger contribution from smoke on the southern part of the average plume.

3.2 Stratiform clouds

The clouds height distributions along the ROI show a bi-modal distribution in the summer and one dominant mode in the winter season (Fig. 7). This can be interpreted as a separation between the marine stratocumulus clouds that are bounded by the shallow MBL (as was observed during the sampling stage) and other stratiform clouds. The low MSc clouds height can be used as a proxy to the MBL top height. Like in the dust case, when analyzing the stratiform cloud height, the best threshold for separation between the clouds modes was determined by looking for the threshold that will show the weakest sensitivity of the average clouds mode height to small threshold changes. Based on this analysis the clouds height distribution were separated at 0.8 km, namely, clouds top height equal and below 0.8 km were considered as the lower clouds, and clouds above 0.8 km as the higher clouds.

4 Discussion and conclusions

In this study we used the CALIOP vertical backscattering profiles to examine the seasonal dust height distribution over the Atlantic Ocean during one summer (2006) and one winter (2006–2007). It shows the average height distribution of the dust plumes over the Atlantic. During the summer, Saharan dust transport over the Atlantic Ocean characterized by two levels of plumes: (a) elevated plumes, mostly separated from the underneath MBL and undercut below by the trade winds and (b) lower plumes, attached and most probably within the MBL. During the winter the bi-modal trend is less clear, since the dust transport occurs in lower altitudes compared to the summer. Over the western parts of the Atlantic Ocean we could not separate the two apparent modes, therefore we assumed that the aerosol are transported in one dust layer that includes the marine mixed layer, in both seasons (in the winter it is a mixed dust-smoke plume).

The average vertical depth of the summer upper dust plumes is 3 to 3.6 km with average top height of 5.1±0.4 km near the African coast (15° W). A decrease in height of 0.028 km per 1° longitude yields dust top height of 3.5 km and a base touching the ocean around 72° W east of the Caribbean Sea.

The winter upper dust and smoke plumes average width is 2 to 2.7 km, with average top height of 3.7±0.4 km near the Gulf of Guinea (10° E). A height slope of 0.02 km per 1° longitude yielding dust-smoke plumes top height of 2.5 km and a base touching the ocean around 50° W, over the Amazon.

Our analysis shows the presence of a lower dust plumes in both seasons with average top heights above the MBL. The average summer lower dust plumes top height is 1.5±0.25 km and it is 1.1±0.35 km in the winter. In both seasons the lower dust plumes top heights slightly increase toward the western side of the Atlantic Ocean.

The stratiform clouds height analysis showed bi-modal distribution as well. The MSc clouds (bounded by the MBL) contribute to the lower clouds at average height less than 0.8 km. The higher (less common) clouds, of other stratiform types, appear mostly in the summer. The presence of the lower dust plumes suggests a direct interaction between the clouds and the dust, as their co-existence was observed at the sampling stage. Moreover, on average, the base of the upper dust plumes will reach height of less than 1 km in longitude of 43° W in the summer and longitude 7° E in the winter, over the Atlantic Ocean where there are still significant amount of MSc cloud fields (Fig. 7).

Acknowledgements. This research was partly funded by the Weizmann-Argentina Cooperation program. I. K. is incumbent of the Benjamin H. Swig and Jack D. Weiler career development chair.

References

Albrecht, B. A.: Aerosols, cloud microphysics, and fractional cloudiness, Science, 245, 1227–1230, 1989.

Anderson, T. L., Charlson, R. J., Bellouin, N., Boucher, O., Chin, M., Christopher, S. A., Haywood, J., Kaufman, Y. J., Kinne, S., Ogren, J. A., Remer, L. A., Takemura, T., Tanre, D., Torres, O., Trepte, C. R., Wielicki, B. A., Winker, D. M., and Yu, H.: A-Train strategy for quantifying direct climate forcing by anthropogenic aerosols, B. Am. Meteorol. Soc., 86, 1795–1809, 2005.

Bergametti, G. and Dulac, F.: Progress and remaining challenges in dust deposition theory and schemes, 3rd International Workshop on Mineral Dust Leipzig, Germany, 15–17 September, 2008.

Carlson, T. N. and Prospero, J. M.:, The large-scale movement of Saharan air outbreaks over the northern equatorial Atlantic, J. Appl. Meteor., 11, 283–297, 1972.

Chiapello, I., Bergametti, G., Gomes, L., Chatenet, B., Dulac, F., Pimenta, J., and Soares, E. S.: An Additional Low Layer Transport of Sahelian and Saharan Dust Over the North-Eastern Tropical Atlantic, Geophys. Res. Lett., 22(23), 3191–3194, 1995.

Dubovik, O., Holben, B., Eck, T. F., Smimov, A., Kaufman, Y. J., King, M. D., Tanré, D., and Slutsker, I.: Variability of absorption and optical properties of key aerosol types observed in worldwide locations, J. Atmos. Sci., 59, 590–608, 2002.

Engelstaedter, S., Washington, R., and Tegen, I.: North African dust emissions and transport, Earth-Sci. Rev., 79(1–2), 73–100, 2006.

Falkowski, P. G., Barber, R. T., and Smetacek, V.: Biogeochemical C ontrols and Feedbacks on Ocean Primary Production, Science, 281, 200–206, 1998.

Formenti, P., Rajot, J. L., Desboeufs, K., Caquineau, S., Chevaillier, S., Nava, S., Gaudichet, A., Journet, E., Triquet, S., Alfaro, S., Chiari, M., Haywood, J. M., Coe, H., and Highwood, E. J.: Regional variability of the composition of mineral dust from Western Africa: results from the AMMA SOP0/DABEX and DODO, J. Geophys. Res, 113, D00C13, doi:10.1029/2008JD009903, 2008.

Garrison, V. H., Shinn, E. A., Foreman, W. T., Griffin, D. W., Holmes, C. M., Kellogg, C. A., Majewski, M. S., Richardson, L. L., Ritchie, K. B., and Smith, G. W.: African and Asian dust: From desert soils to coral reefs, Bioscience, 53, 469–480, 2003.

Generoso, S., Bey, I., Labonne, M., and Bréon, F. M.: Aerosol vertical distribution in dust outflow over the Atlantic: Comparisons between GEOS-Chem and Cloud-Aerosol Lidar and Infrared Pathfinder Satellite Observation (CALIPSO), J. Geophys. Res., 113, D24209, doi:10.1029/2008JD010154, 2008.

Hansen, J., Sato, M., and Ruedy, R.: Radiative forcing and climate response, J. Geophys. Res., 102(D6), 6831–6864, 1997.

Herman, J. R., Bhartia, P. K., Torres, O., Hsu, C., Seftor, C., and Celarier, E.: Global distribution of UV-absorbing aerosols from Nimbus-7/TOMS data, J. Geophys. Res., 102(D6), 6831–6864, 1997.

IPCC: Climate Change 2007: The Scientific Basis. Contribution of Working Group I to the fourth Assessment Report of the Intergovernmental Panel on Climate Change, edited by: Solomon, S., Qin, D., Manning, M., Chen, Z., Marquis, M., Averyt, K. B., Tignor, M., and Miller, H. L., Cambridge University Press, Cambridge, United Kingdom and New York, NY, USA, 996 pp., 2007.

Israelevich, P. L., Levin, Z., Joseph, J. H., and Ganor, E.: Desert aerosol transport in the Mediterranean region as inferred from the TOMS aerosol index, J. Geophys. Res., 107(D21), 4572, doi:10.1029/2001JD002011, 2002.

Karyampudi, V. M. and Carlson, N. T.: Analysis and numerical simulations of the Saharan Air Layer and its effect on easterly wave disturbances, J. Atmos. Sci., 45(21), 3102–3136, 1988.

Karyampudi, V. M., Palm, S. P., Reagen, J. A., Fang, H., Grant, W. B., Hoff, R. M., Moulin, C., Pierce, H. F., Torres, O., Browell, E. V., and Melfi, S. H.: Validation of the Saharan dust plume conceptual model using lidar, Meteosat and ECMWF, B. Am. Meteorol. Soc., 80, 1045–1075, 1999.

Kaufman, Y. J., Tanre D., and Boucher O.: A satellite view of aerosols in the climate system, Review. Nature, 419, 215–223, 2002.

Kaufman, Y. J., Koren, I., Remer, L. A., Rosenfeld, D., and Rudich, Y.: The Effect of Smoke, Dust and Pollution Aerosol on Shallow Cloud Development Over the Atlantic Ocean, Proceedings of the National Academy of Sciences, 102(32), 11207–11212, 2005a.

Kaufman, Y. J., Koren, I., Remer, L. A., Tanre, D., Ginoux, P., and Fan, S.: Dust transport and deposition observed from the Terra-Moderate Resolution Imaging Spectroradiometer (MODIS) spacecraft over the Atlantic Ocean, J. Geophys. Res., 110, D10S12, doi:10.1029/2003JD004436, 2005b.

Kaufman, Y. J., Boucher, O., Tanre, D., Chin, M., Remer, L. A., and Takemura, T.: Aerosol anthropogenic component estimated from satellite data, Geophys. Res. Lett., 32, L17804, doi:10.1029/2005GL023125, 2005c.

Koren, I., Kaufman, Y. J., Rosenfeld, D., Remer, L. A., and Rudich, Y.: Aerosol invigoration and restructuring of Atlantic convective clouds, Geophys. Res. Lett., 32, LI4828, doi: 10.1029/2005GL023187, 2005.

Koren, I., Kaufman, Y. J., Washington, R., Todd, C. C., Rudich, Y., Martins, J. V., and Rosenfeld, D.: The Bod'el'e depression: a single spot in the Sahara that provides most of the mineral dust to the Amazon forest, Environ. Res., 1, 1–5, 2006.

Levin, Z., Ganor, E., and Gladstein, V.: The effects of desert particles coated with sulfate on rain formation in the eastern Mediterranean, J. Appl. Meteor., 35, 1511–1523, 1996.

Liu, Z., Liu, D., Huang, J., Vaughan, M., Uno, I., Sugimoto, N., Kittaka, C., Trepte, C., Wang, Z., Hostetler, C., and Winker, D.: Airborne dust distributions over the Tibetan Plateau and surrounding areas derived from the first year of CALIPSO lidar observations, Atmos. Chem. Phys., 8, 5045–5060, 2008, http://www.atmos-chem-phys.net/8/5045/2008/.

Middleton, N. J. and Goudie, A. S.: Saharan dust: sources and trajectories, Transactions of the Institute of British Geographers, 26(2), 165–181, 2001.

Psenner, R.: Living in a dusty world: airborne dust as a key factor for alpine lakes, Water, Air and Soil Pollution, 112(3–4), 217–227, 1999.

Prospero, J. M. and Carlson, T. N.: Vertical and areal distribution of Saharan dust over the western equatorial North Atlantic ocean, J. Geophys. Res., 77 5255–65, 1972.

Prospero, J. M. and Nees R. T.: Dust concentration in the atmosphere of the equatorial North Atlantic: Possible relationship to the Sahelian drought, Science, 196, 1196–1198, doi:10.1126/science.196.4295.1196, 1977.

Prospero, J. M., Ginoux, P., Torres, O., Nicholson, S. E., and Gill, T. E.: Environmental characterization of global sources of atmospheric soil dust identified with the NIMBUS 7 total ozone mapping spectrometer (TOMS) absorbing aerosol product, Rev. Geophys., 40, 1002, doi:10.1029/2000RG000095, 2002.

Prospero, J. M. and Lamb, J. P.: African droughts and dust transport to the Caribbean: Climate change and implications, Science, 302, 1024–1027, 2003.

Ramanathan, V., Crutzen, P. J., Kiehl, J. T., and Rosenfeld, D.: Aerosols, climate, and the hydrological cycle, Science, 294, 2119–2124, 2001.

Reichholf, J. H.: Is Saharan dust a major source of nutrients for the Amazonian rain forest?, Studies on Neotropical Fauna and Environment, 21(4), 251–255, 1986.

Swap, R., Garstang, M., Greco, S., Talbot, R., and Kallberg, P.: Saharan dust in Amazon basin, Tellus, 44B, 133–149, 1992.

Tanaka, T. Y.: Dust emission and deposition in global models Meteorological Research Institute, 3rd International Workshop on Mineral Dust Leipzig, Germany, 15–17 September, 2008.

Twomey, S.: Pollution and the planetary albedo, Atmos. Environ., 8, 1251–1256, 1974.

Vaughan, M., Young, S., Winker, D., Powell, K., Omar, A., Liu, Z., Hu, Y., and Hostetler, C.: Fully

Automated Analysis of Space-based Lidar data: an Overview of the CALIPSO Retrieval Algorithms and Data Products, Proc. SPIE Laser Radar Techniques for Atmospheric Sensing, 5575, 16–30, 2004.

Wendisch, M., Bierwirth, E., Bauer, S., Otto, S., and Trautmann, T.: Major Factors Influencing Local Dust Radiative Forcing, 3rd International Workshop on Mineral Dust Leipzig, Germany, 15–17 September, 2008.

Winker, D. M. and Pelon, J.: The CALIPSO mission, Geoscience and Remote Sensing Symposium, 2003, IGARSS '03. Proceedings. IEEE International, 2, 1329–1331, 2003.

Winker, D. M., Hunt, W. H., and McGill, M. J.: Initial performance assessment of CALIOP, Geophys. Res. Lett., 34, L19803, doi:10.1029/2007GL030135, 2007.

Yu, H., Kaufman, Y. J., Chin, M., Feingold, G., Remer, L., Anderson, T., Balkanski, Y., Bellouin, N., Boucher, O., Christopher, S., DeCola, P., Kahn, R., Koch, D., Loeb, N., Reddy, M. S., Schulz, M., Takemura, T., and Zhou, M.: A review of measurement-based assessments of aerosol direct radiative effect and forcing, Atmos. Chem. Phys., 6, 613–666, 2006, http://www.atmos-chem-phys.net/6/613/2006/.

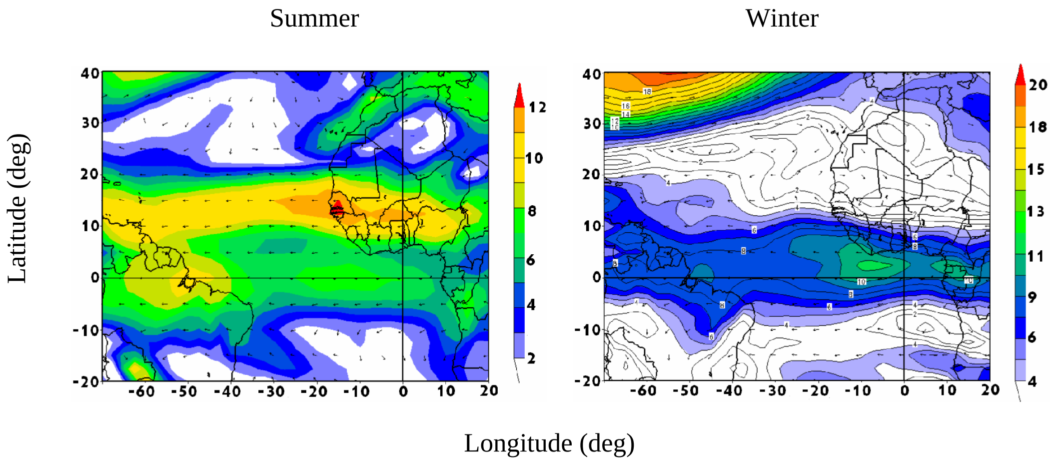

Fig. 1. 700 mb level winds (m s^{-1}) for the the summer (June–August 2006) and winter (December 2006–February 2007) based on National Center for Environmental Prediction (NCEP) re-analysis.

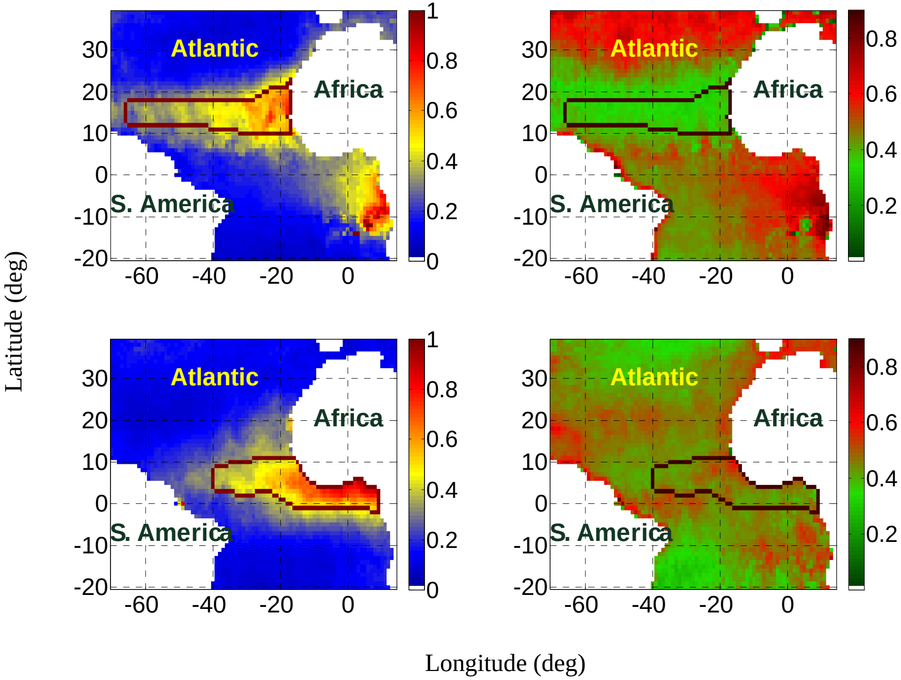

Fig. 2. Aerosol optical properties over the Atlantic Ocean, for the 2006 summer (upper row) and 2006–2007 winter (lower row), from the MODIS instrument onboard Terra. Left column: the aerosol optical depth (at 550 nm). Right column: the aerosol fine mode fraction. The contours mark the center of the seasonal plume.

Title Page
Abstract
Introduction
Conclusions
References
Tables
Figures
◀◀
▶▶
◀
▶
Back
Close
Full Screen / Esc
Printer-friendly Version
Interactive Discussion

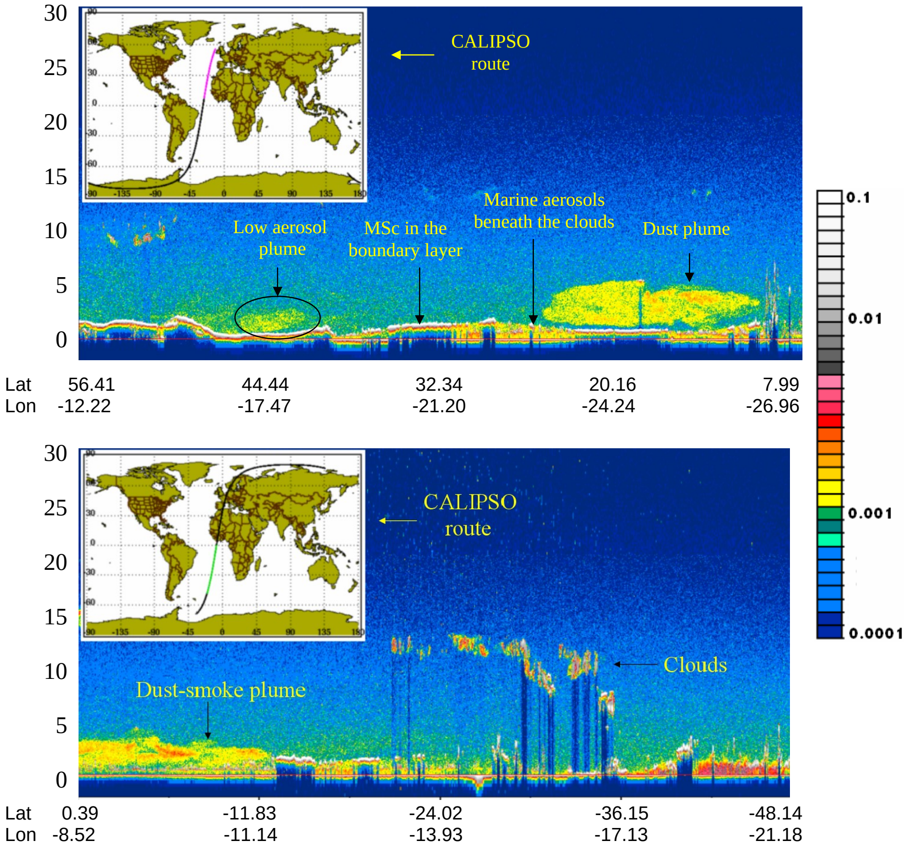

Fig. 3. CALIPSO summer (upper part, 6 July 2006) versus winter (lower part, 4 February 2007) nocturnal vertical attenuated backscatter (in km^{-1} sr^{-1}). X axis: latitude (upper scale) and longitudes (lower scale). The internal figures present the routes of the satellite.

Title Page

Abstract | Introduction

Conclusions | References

Tables | Figures

◀| |▶

◀ ▶

Back | Close

Full Screen / Esc

Printer-friendly Version

Interactive Discussion

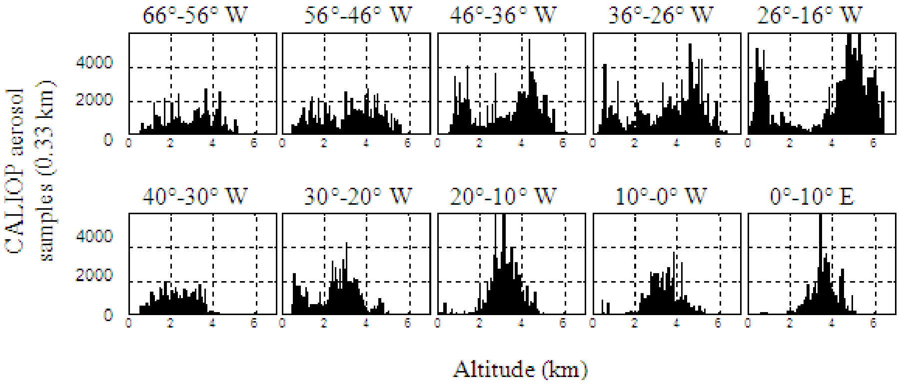

Fig. 4. Aerosol plumes top height distribution (for all CALIOP samples and before excluding the MBL tops) along the center of the plumes (see Fig. 2), for the summer (upper row) and winter (lower row). Each histogram covers an area of 10° longitudes along the contour line (marked in Fig. 2), starting from the West North African coastline (right) toward the Americas (left). Samples for horizontal intervals of 330 m along the flight track.

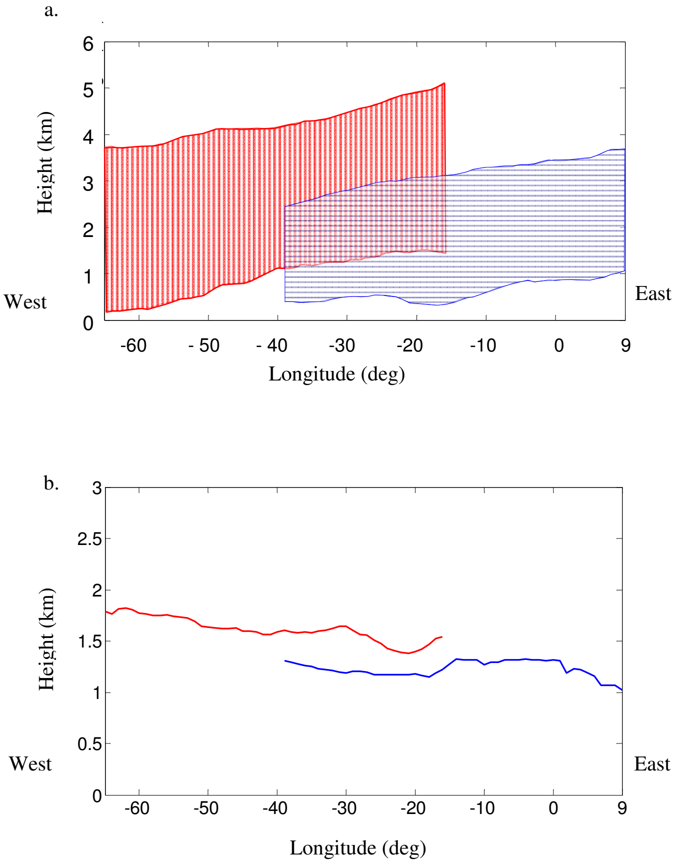

Fig. 5. Results of **(a)** the average dust height and thickness of the summer (red) and winter (blue) upper plumes, and **(b)** the average lower dust plumes top heights. All averages were calculated along the ROI, and after determination of the best thresholds.

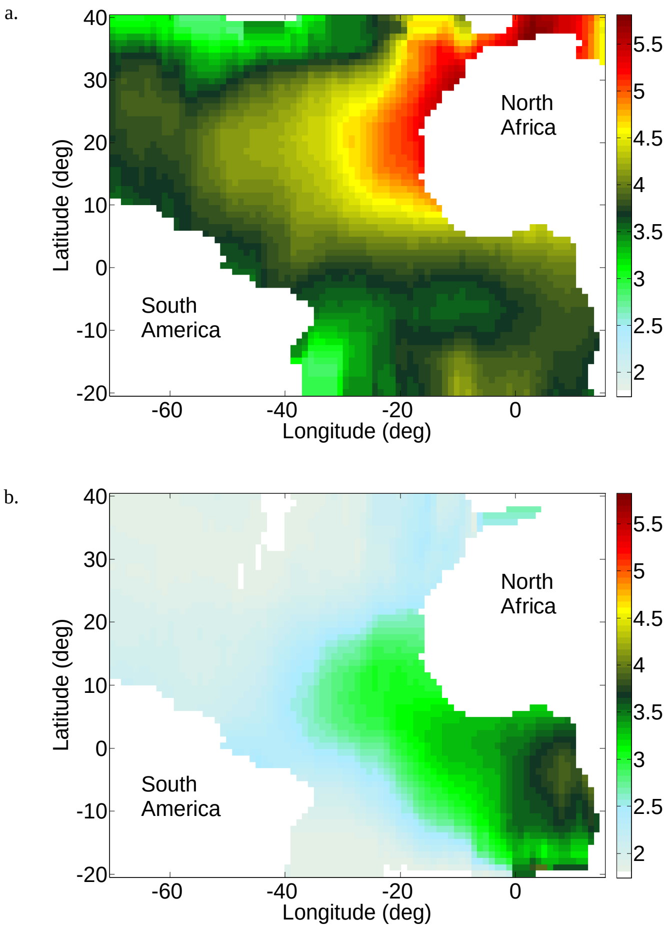

Fig. 6. Averaged seasonal spatial distribution of the upper dust plums top height for **(a)** the summer and **(b)** winter seasons; scale height in km.

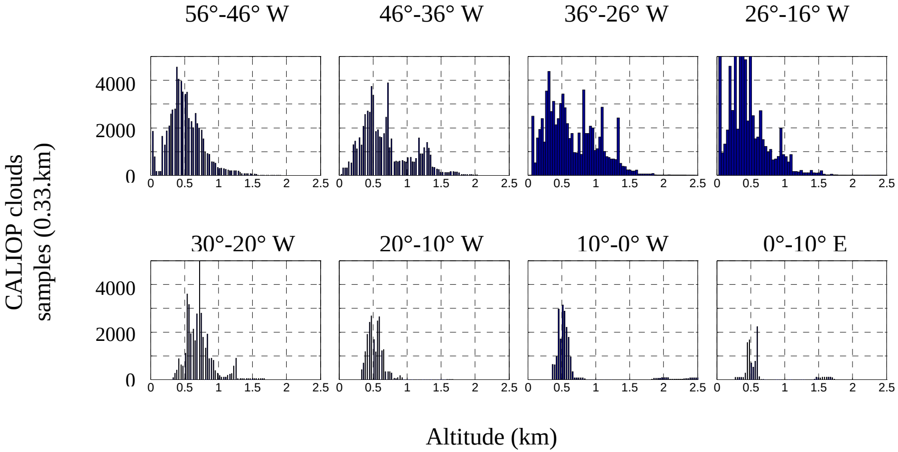

Fig. 7. Clouds top height distribution (for all CALIOP samples) along the ROI, for the summer (upper panel) and winter (lower panel). Each histogram covers an area of 10° longitudes along the contour line (marked in Fig. 2), starting from the West North African coastline (right) toward the Americas (left). Samples for horizontal intervals of 330 m along the flight track.